

Control Synthesis Along Uncertain Trajectories Using Integral Quadratic Constraints*

Felix Biertümpfel¹, Peter Seiler² and Harald Pfifer¹

Abstract—The paper presents a novel approach to synthesize robust controllers for nonlinear systems along perturbed trajectories. The approach linearizes the system with respect to a reference trajectory. In contrast to existing methods rooted in robust linear time-varying synthesis, the approach accurately includes perturbations that drive the system away from the reference trajectory. Hence, the controller obtained in the linear framework provides a significantly more robust nonlinear performance. The calculation of the controller is derived from robust synthesis approaches rooted in the integral quadratic constraints framework. The feasibility of the approach is demonstrated on a pitch tracker design for a space launcher.

I. INTRODUCTION

Following a predefined trajectory is a fundamental engineering problem, e.g. for robotic manipulators [1], space launch vehicles [2], and planetary landers [3]. Uncertainties and disturbances can cause the system to diverge from the predefined trajectory and degrade their performance. For instance, the ascent trajectory of a space launcher is determined for a certain wind profile and will differ substantially for any variation in the wind. Thus, a controller must provide robustness against omnipresent trajectory perturbations.

System dynamics are usually modeled by nonlinear differential equations. The nonlinear differential equations can be linearized with respect to a reference trajectory yielding a finite horizon linear time-varying (LTV) system. Its system matrices are known functions of time and resemble the original system dynamics. There are various approaches in the literature to synthesize controllers for LTV systems. These include methods for nominal synthesis [4], [5] and robust synthesis for systems with uncertainty [6]–[8]. Most recent synthesis approaches for robust controllers reside inside the integral quadratic constraint (IQC) framework [9], which is briefly presented in Section II. However, the synthesis approaches so far only consider uncertainties in the LTV state space representation. They thus fail to recover the dynamics of the nonlinear system if parameters are perturbed along the trajectory.

The present paper extends the LTV robust synthesis framework in [9] to robust controllers for nonlinear systems in the vicinity of a reference trajectory. To do so, the state

space representation of the LTV system is extended with a constant driving term and terms associated with the parameter variations in Section III. Specifically, the synthesis problem is shown in Section IV to become a LTV IQC synthesis under uncertain initial conditions. Furthermore, the effects of the linearization error along the trajectory can be included in a similar way, see, e.g., [10]. Thus, a robust controller for nonlinear systems along uncertain trajectories can be calculated using linear methods. The approach is demonstrated on a pitch tracker control design of space launcher in Section V.

II. PRELIMINARIES

A. Uncertain Linear Time-Varying Systems

An uncertain linear time-varying system $\mathcal{F}_u(N, \Delta)$ is defined by the feedback interconnection of a nominal LTV system N and the perturbation Δ , also referred to as “uncertainty” for simplicity, as pictured in Fig. 1.

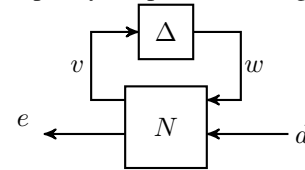


Fig. 1: Interconnection LTV system N and uncertainty Δ . The known LTV system N is given by:

$$\begin{bmatrix} \dot{x}(t) \\ v(t) \\ e(t) \end{bmatrix} = \begin{bmatrix} A(t) & B_w(t) & B_d(t) \\ C_v(t) & D_{vw}(t) & D_{vd}(t) \\ C_e(t) & D_{ew}(t) & D_{ed}(t) \end{bmatrix} \begin{bmatrix} x(t) \\ w(t) \\ d(t) \end{bmatrix} \quad (1)$$

In (1), $x(t) \in \mathbb{R}^{n_x}$, $d(t) \in \mathbb{R}^{n_d}$, and $e(t) \in \mathbb{R}^{n_e}$ denote the state, input, and the output vector, respectively. The vectors $w(t)$ and $v(t)$ connect N with Δ , i.e., $w = \Delta(v)$. The state space matrices are piecewise continuous locally bounded matrix-valued functions of time with corresponding dimensions. To shorten the notation, the explicit time dependence is omitted, if clear from the context. The uncertainty $\Delta : L_2^{n_v}[0, T] \rightarrow L_2^{n_w}[0, T]$ is a bounded and causal operator. The interconnection $\mathcal{F}_u(N, \Delta)$ in Fig. 1 is said to be well-posed if, for all initial conditions, $x(0)$ and $d \in L_2[0, T]$ unique solutions $x \in L_2[0, T]$, $v \in L_2[0, T]$, and $w \in L_2[0, T]$ satisfying (1) and causally dependent on d exist.

Let \mathcal{S} denote a set of uncertainties to be considered. The robust performance of the uncertain system $\mathcal{F}_u(N, \Delta)$ for uncertain initial conditions and a given Δ is quantified by

$$\|\mathcal{F}_u(N, \Delta)\|_{2[0, T]} := \sup_{\substack{d \in L_2[0, T] \\ d \neq 0, x(0) \in \mathbb{R}^{n_x}}} \left[\frac{\|e\|_{2[0, T]}^2}{\|d\|_{2[0, T]}^2 + \|x(0)\|_2^2} \right]^2, \quad (2)$$

*This work was supported by the European Union under Grant No. 101153910. The responsibility for the content of this paper is with its authors.

¹ Felix Biertümpfel and Harald Pfifer are with the Chair of Flight Mechanics and Control, Technische Universität Dresden, 01069 Dresden, Germany felix.biertuempfel@tu-dresden.de harald.pfifer@tu-dresden.de

² Peter Seiler is with the Department of Electrical and Computer Engineering at the University of Michigan, Ann Arbor, pseiler@umich.edu

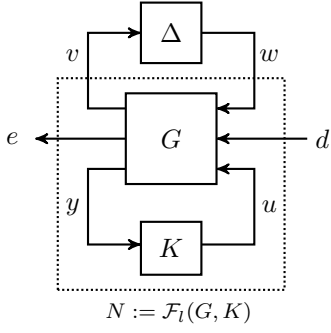


Fig. 2: Uncertain closed loop $\mathcal{F}_u(\mathcal{F}_l(G, K), \Delta)$

where $\|d\|_{2[0,T]} := \left[\int_0^T d(t)^T d(t) dt \right]^{\frac{1}{2}}$ is the L_2 norm on the finite horizon $[0, T]$. The worst-case gain over the uncertainty set is $\sup_{\Delta \in \mathcal{S}} \|\mathcal{F}_u(N, \Delta)\|_{2[0,T]}$.

The input/output behavior of Δ is bounded via time-domain IQCs. Time-domain IQCs are defined by a filter $\Psi \in \mathbb{RH}_{\infty}^{n_z \times (n_v + n_w)}$ with input $[v^T, w^T]^T$ and output z , and a $n_z \times n_z$ real, symmetric matrix M , see, e.g., [11]. The uncertainty Δ satisfies the time domain IQC defined by M and Ψ if the filter output z fulfills $\int_0^T z(t)^T M z(t) dt \geq 0$ for all $v \in L_2[0, T]$, $w = \Delta(v)$ over the interval $[0, T]$ for zero initial conditions. In this case, the short notation $\Delta \in \text{IQC}(\Psi, M)$ is used. An example for feasible parameterization and factorization of a time-varying parametric uncertainty is given below.

Example 1: Let \mathcal{S} denote the set of nonlinear, time-varying, uncertainties with a given norm-bound b , i.e. $\Delta \in \mathcal{S}$ if $\|\Delta\|_{2 \rightarrow 2, [0, T]} \leq b$. If $\Delta \in \mathcal{S}$, then for any constant $\lambda \geq 0$ it satisfies the IQC defined by the static filter $\Psi = I_{n_v + n_w}$ and constant matrix:

$$M := \begin{bmatrix} b^2 \lambda I_{n_v} & 0 \\ 0 & -\lambda I_{n_w} \end{bmatrix}$$

B. Robust Synthesis

Fig. 2 shows the feedback interconnection $\mathcal{F}_u(\mathcal{F}_l(G, K), \Delta)$ of an uncertain LTV system and the controller K , with $N := \mathcal{F}_l(G, K)$ corresponding to (1). The finite horizon robust synthesis problem is to find a linear time-varying controller simultaneously minimizing the impact of worst-case disturbances and worst-case uncertainties, i.e.:

$$\inf_K \sup_{\Delta \in \mathcal{S}} \|\mathcal{F}_u(\mathcal{F}_l(G, K), \Delta)\|_{2[0, T]} \quad (3)$$

In general, problem (3) is non-convex. Reference [9] provides an iterative approach to synthesize a robust LTV controller for zero initial conditions. Particularly, the procedure iterates through three essential steps: 1) Construction of the scaled plant using the IQC data (Ψ, M) , 2) Nominal LTV synthesis using the scaled plant, and 3) IQC-based robust performance analysis of the uncertain closed loop $\mathcal{F}_u(\mathcal{F}_l(G, K), \Delta)$. The steps are briefly presented in the following and the reader is referred to [9] for more detailed explanations.

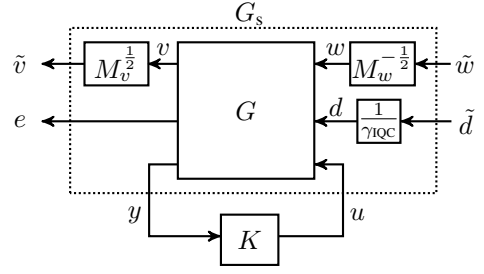


Fig. 3: Scaled Plant G_s

1) *Scaled Plant Construction:* The scaled plant $G_s^{(i)}$ at an iteration step i is constructed as shown in Fig. 3 by scaling the performance and uncertainty channels of G using $M_v^{(i-1)}$, $M_w^{(i-1)}$ and the worst case upper bound $\gamma_{\text{IQC}}^{(i-1)}$ from the previous iteration or user-specified initial values for the first iteration. This scaling ensures appropriate normalization of the performance and uncertainty channels. This is a key step which connects the nominal synthesis (step 2) and worst-case gain problem (step 3). Let the uncertain plant (1) be given as shown in Fig. 1. The superscripts $(i-1)$ are dropped in the following for better readability. The IQC matrix is assumed constant with the particular form $M = \text{diag}\{M_v, -M_w\}$ where $M_v > 0$ and $M_w > 0$. Time-varying IQC-matrices are not pursued in this paper, but are covered in, e.g., [9]. Additionally, the worst-case gain bound scales the corresponding disturbance channel $\tilde{d} = \gamma_{\text{IQC}}^{(i-1)} d$. The scaled plant G_s is constructed as shown in Fig. 3. The scaled plant has nominal performance $\|G_s\|_{2[0, T]} \leq 1$.

2) *Nominal Synthesis:* The next step is to perform finite horizon nominal synthesis on the scaled plant. This step is performed using a special case of the synthesis results described in [12]. This yields a controller $K^{(i)}$ minimizing the induced norm from $[\tilde{w}^T, \tilde{d}^T]^T$ to $[\tilde{v}^T, e^T]$.

3) *IQC Analysis:* Finally, the the worst-case gain upper bound $\gamma_{\text{IQC}}^{(i)}$ of the uncertain closed loop $\mathcal{F}_u(\mathcal{F}_l(G, K), \Delta)$ is computed. Note that this step uses the original uncertain plant without any scalings. A differential linear matrix inequality (DLMI) can be used to calculate an upper bound on the worst-case gain. Theorem 6 in Reference [13] states a sufficient DLMI condition to bound the worst case performance. The corresponding algorithm is used in [9] to calculate $\gamma_{\text{IQC}}^{(i)}$. All subsequent iterations require the construction of a scaled plant using the IQC results and ultimately links the analysis and synthesis step.

III. PROBLEM FORMULATION

Consider a nonlinear system \tilde{N} whose dynamics are defined by the nonlinear ordinary differential equations (ODEs)

$$\begin{aligned} \dot{x}(t) &= f(x(t), d(t), u(t), \rho(t)) \\ e(t) &= h(x(t), d(t), u(t), \rho(t)) \\ y(t) &= g(x(t), d(t), u(t), \rho(t)). \end{aligned} \quad (4)$$

In (4), the vector $\rho(t) \in \mathbb{R}^{n_\rho}$ denotes a time-varying parameter vector at time t . A pre-defined trajectory is defined

as a unique solution of (4) satisfying

$$\begin{aligned} \dot{x}_{\mathcal{T}}(t) &= f(x_{\mathcal{T}}(t), d_{\mathcal{T}}(t), u_{\mathcal{T}}(t), \rho_{\mathcal{T}}(t)) \\ e_{\mathcal{T}}(t) &= h(x_{\mathcal{T}}(t), d_{\mathcal{T}}(t), u_{\mathcal{T}}(t), \rho_{\mathcal{T}}(t)) \\ y_{\mathcal{T}}(t) &= g(x_{\mathcal{T}}(t), d_{\mathcal{T}}(t), u_{\mathcal{T}}(t), \rho_{\mathcal{T}}(t)) \quad \forall t \in [0, T]. \end{aligned} \quad (5)$$

The subscript \mathcal{T} will be used to denote a specific trajectory, $(x_{\mathcal{T}}, d_{\mathcal{T}}, u_{\mathcal{T}}, \rho_{\mathcal{T}})$ satisfying (5). The objective of the paper is to design a controller K , which in feedback interconnection with the system \tilde{N} (4) satisfies given performance requirements along a prescribed trajectory over the finite time horizon $[0, T]$. The resulting closed loop system denoted by $\mathcal{F}_l(\tilde{N}, K)$ shall be robust against perturbations in both the input signal d_{Δ} and parameter signal ρ_{Δ} :

$$d_{\Delta} := d - d_{\mathcal{T}}, \quad \rho_{\Delta} := \rho - \rho_{\mathcal{T}}. \quad (6)$$

The parameter perturbation ρ_{Δ} is confined, at each point in time, to a set $\mathcal{P} \subseteq \mathbb{R}^{n_{\rho}}$.

Defining a robust performance certificate for the control design process of a nonlinear closed loop is difficult. The alternative is to synthesize a robust controller using methods for finite horizon LTV systems. This requires a linearization of (4) via Taylor series expansion of f , h , and g about the reference trajectory \mathcal{T} . Define $x_{\Delta}(t) := x(t) - x_{\mathcal{T}}(t)$ and $u_{\Delta}(t) := u(t) - u_{\mathcal{T}}(t)$. The expansion is

$$\begin{aligned} \dot{x} &= \dot{x}_{\mathcal{T}} + \underbrace{\frac{\partial f}{\partial x}}_{C_e} \Big|_{\mathcal{T}} x_{\Delta} + \underbrace{\frac{\partial f}{\partial d}}_{D_{ed}} \Big|_{\mathcal{T}} d_{\Delta} + \underbrace{\frac{\partial f}{\partial u}}_{D_{eu}} \Big|_{\mathcal{T}} u_{\Delta} + \underbrace{\frac{\partial f}{\partial \rho}}_{F_e} \Big|_{\mathcal{T}} \rho_{\Delta} + \epsilon_f \\ e &= e_{\mathcal{T}} + \underbrace{\frac{\partial h}{\partial x}}_{C_y} \Big|_{\mathcal{T}} x_{\Delta} + \underbrace{\frac{\partial h}{\partial d}}_{D_{yd}} \Big|_{\mathcal{T}} d_{\Delta} + \underbrace{\frac{\partial h}{\partial u}}_{D_{yu}} \Big|_{\mathcal{T}} u_{\Delta} + \underbrace{\frac{\partial h}{\partial \rho}}_{F_y} \Big|_{\mathcal{T}} \rho_{\Delta} + \epsilon_h, \\ y &= y_{\mathcal{T}} + \underbrace{\frac{\partial g}{\partial x}}_{C_y} \Big|_{\mathcal{T}} x_{\Delta} + \underbrace{\frac{\partial g}{\partial d}}_{D_{yd}} \Big|_{\mathcal{T}} d_{\Delta} + \underbrace{\frac{\partial g}{\partial u}}_{D_{yu}} \Big|_{\mathcal{T}} u_{\Delta} + \underbrace{\frac{\partial g}{\partial \rho}}_{F_y} \Big|_{\mathcal{T}} \rho_{\Delta} + \epsilon_g. \end{aligned} \quad (7)$$

Here, ϵ_f , ϵ_h , and ϵ_g denote higher-order terms in the Taylor expansion. Moreover, $\frac{\partial f}{\partial x} \Big|_{\mathcal{T}}$ denotes the Jacobian of f with respect to x evaluated along \mathcal{T} . The common LTV state space representation neglects the higher order terms ϵ_f , ϵ_h , ϵ_g , and assumes nominal parameters, i.e., $\rho_{\Delta}(t) = 0$ for $t \in [0, T]$. This approximation \bar{N} is equivalent to the LTV system \bar{N} in (1) for $v = w = 0$, and additional input u and output y .

A performance metric for $\mathcal{F}_l(\bar{N}, K)$ can be defined as

$$\sup_{\substack{d_{\Delta} \in L_2[0, T] \\ d_{\Delta} \neq 0, x_{\Delta}(0) = 0}} \frac{\|e_{\Delta}\|_{2[0, T]}}{\|d_{\Delta}\|_{2[0, T]}}, \quad (8)$$

which is, in fact, the nominal formulation of (2). A controller K minimizing the closed loop gain can be readily synthesized for such a system using the results in, e.g., [4]. The gain (8) relates perturbations in the input to perturbations from the nominal output $e_{\mathcal{T}}$ with respect to their $L_2[0, T]$ norm. Since the reference output is known and $\|e\|_{2[0, T]} \leq \|e_{\mathcal{T}}\|_{2[0, T]} + \|e_{\Delta}\|_{2[0, T]}$. The result can, in principle, be used to establish an upper bound on the performance of

the nonlinear closed loop. However, no actual performance guarantees are provided as this synthesis does not consider parameter perturbations and further neglects the higher-order terms of the Taylor series expansion

Remark 1: In an attempt to cover the effects of perturbations and linearization errors, uncertainties Δ are typically added in LFT fashion to the nominal LTV system \bar{N} , i.e., $\mathcal{F}_u(\bar{N}, \Delta)$, as seen in Section II. The resulting uncertain LTV system equals (1). A robust controller can be synthesized following the approach described in Section II. However, the signal injected into Δ remains zero as long as d_{Δ} is zero. Hence uncertainty modeled in this way cannot, on its own, drive states away from the nominal trajectory. This contradicts the behavior of the nonlinear system (4), where a parameter perturbation ρ_{Δ} is enough to drive the system away from the reference trajectory. Thus, the controller provides no robustness against trajectory perturbations. Alternatively, the parameter variation can be treated as an external disturbance, see, e.g., [2]. However, this limits the perturbation to be part of the norm-bounded input signal d_{Δ} .

IV. SYNTHESIS ALONG UNCERTAIN TRAJECTORIES

A. Synthesis Problem

Unlike the common approach described so far, the synthesis in this paper explicitly considers perturbations from the reference trajectory, i.e., $\rho_{\Delta}(t) \neq 0$. Hence, it can be used to synthesize a controller providing robust performance of the nonlinear closed loop system. The linearization errors ϵ_f , ϵ_h , and ϵ_g are not explicitly considered, to make the section more lucid. However, they can be included into the synthesis following the same steps as for ρ_{Δ} . Details are provided in [10].

An alternative state space representation of (7) is obtained by extending the state vector x_{Δ} with a constant driving term:

$$\begin{aligned} \begin{bmatrix} \dot{x}_{\Delta} \\ 0 \end{bmatrix} &= \begin{bmatrix} A & E\rho_{\Delta} \\ 0 & 0 \end{bmatrix} \begin{bmatrix} x_{\Delta} \\ 1 \end{bmatrix} + \begin{bmatrix} B_d & B_u \\ 0 & 0 \end{bmatrix} \begin{bmatrix} d_{\Delta} \\ u_{\Delta} \end{bmatrix} \\ \begin{bmatrix} e_{\Delta} \\ y_{\Delta} \end{bmatrix} &= \begin{bmatrix} C_e & F_e\rho_{\Delta} \\ C_y & F_y\rho_{\Delta} \end{bmatrix} \begin{bmatrix} x_{\Delta} \\ 1 \end{bmatrix} + \begin{bmatrix} D_{ed} & D_{eu} \\ D_{yd} & D_{yu} \end{bmatrix} \begin{bmatrix} d_{\Delta} \\ u_{\Delta} \end{bmatrix} \end{aligned} \quad (9)$$

This model is equivalent to (7). However, (9) is non-standard due to the constant driving term extending the original state vector. This reformulation, however, enables parameter variations to excite the system dynamics even if no external disturbances occur. The next step is to replace the driving term by a (scalar) pseudo-state $x_{\rho} := 1$ yielding the extended system:

$$\begin{aligned} \begin{bmatrix} \dot{x}_{\Delta} \\ 0 \end{bmatrix} &= \begin{bmatrix} A & E\rho_{\Delta} \\ 0 & 0 \end{bmatrix} \begin{bmatrix} x_{\Delta} \\ x_{\rho} \end{bmatrix} + \begin{bmatrix} B_d & B_u \\ 0 & 0 \end{bmatrix} \begin{bmatrix} d_{\Delta} \\ u_{\Delta} \end{bmatrix} \\ \begin{bmatrix} e_{\Delta} \\ y_{\Delta} \end{bmatrix} &= \begin{bmatrix} C_e & F_e\rho_{\Delta} \\ C_y & F_y\rho_{\Delta} \end{bmatrix} \begin{bmatrix} x_{\Delta} \\ x_{\rho} \end{bmatrix} + \begin{bmatrix} D_{ed} & D_{eu} \\ D_{yd} & D_{yu} \end{bmatrix} \begin{bmatrix} d_{\Delta} \\ u_{\Delta} \end{bmatrix} \end{aligned} \quad (10)$$

Recall that the parameter perturbations ρ_{Δ} are confined to lie in a compact set \mathcal{P} . Confining the term $\rho_{\Delta}(t)$ to its set allows us to treat it as an uncertainty Δ providing an uncertain LTV system given by the known state space model \hat{N} :

$$\begin{aligned} \begin{bmatrix} \dot{x}_{\Delta}(t) \\ 0 \\ v(t) \\ e_{\Delta}(t) \\ y_{\Delta}(t) \end{bmatrix} &= \begin{bmatrix} A(t) & 0 & E(t) & B_d(t) & B_u(t) \\ 0 & 0 & 0 & 0 & 0 \\ 0 & 1 & 0 & 0 & 0 \\ C_e(t) & 0 & F_h(t) & D_{ed}(t) & D_{eu}(t) \\ C_y(t) & 0 & F_g(t) & D_{yd}(t) & D_{yu}(t) \end{bmatrix} \begin{bmatrix} x_{\Delta}(t) \\ x_{\rho} \\ w(t) \\ d_{\Delta}(t) \\ u_{\Delta}(t) \end{bmatrix} \\ w &= \text{diag}(\rho_{\Delta})v. \end{aligned} \quad (11)$$

For a given controller, the performance of the closed loop system $\mathcal{F}_u(\mathcal{F}_L(\hat{N}, K), \Delta)$ can be quantified by (2). Recall that the pseudo-state x_ρ requires a non-zero initial condition to take effect, but “actual” state variables x_Δ have zero initial conditions. $\mathcal{F}_u(\mathcal{F}_L(\hat{N}, K), \Delta)$ together with the nominal output provides an upper bound for the robust performance of the nonlinear closed loop system $F_l(\hat{N}, K)$. Moreover, it allows to state a synthesis problem calculating an LTV controller minimizing the upper bound on the worst-case closed loop performance:

$$\inf_K \sup_{\Delta \in \mathcal{P}} \|\mathcal{F}_u(\mathcal{F}_l(\hat{N}, K), \Delta)\|_{2[0, T]} \quad (12)$$

This synthesis problem can be solved as a robust LTV synthesis following the steps in II-B. However, the synthesis of a robust LTV controller for a nonlinear system along a perturbed trajectory requires partially non-zero initial conditions in the nominal synthesis and robust performance step, respectively.

B. Computational Approach

The pseudo-code in Algorithm 1 describes the synthesis of an LTV controller for a nonlinear system along an uncertain trajectory.

Algorithm 1 Uncertain Trajectory Synthesis

- 1: **Input:** \hat{N} , i_{\max} , $M_v^{(0)}$, $M_w^{(0)}$, $\gamma_{\text{IQC}}^{(0)}$
 - 2: **Output:** $\gamma_{\text{IQC}}^{(i)}$, $K^{(i)}$
 - 3: **for** $i = 1 : i_{\max}$ **do**
 - 4: **Step 1:** Build scaled plant G_s (Fig. 3) from \hat{N} , $M_w^{(i-1)}$, $M_v^{(i-1)}$, and $\gamma_{\text{IQC}}^{(i-1)}$
 - 5: **Step 2:** Synthesize $K^{(i)}$ for G_s with uncertain initial pseudo state x_ρ and ρ_Δ set to b_ρ
 - 6: **Step 3:** LTV IQC analysis of closed loop with uncertain initial pseudo state x_ρ and uncertain ρ_Δ using $K^{(i)}$ yielding robust performance $\gamma_{\text{IQC}}^{(i)}$, $M_w^{(i-1)}$, and $M_v^{(i-1)}$
 - 7: **end for**
-

A user-defined amount of iterations i_{\max} is provided to the algorithm together with the system \hat{N} (11), with the additional input u and output y . The uncertainty covering the parameter variation $\Delta := \text{diag}(\rho_\Delta)$ is described by \mathcal{S} with its input/output behavior bounded by the IQC in Example 1. Its norm bound is denoted b_ρ . Initial values of the scalings $M_v^{(0)} := I_{n_v}$, $M_w^{(0)} := I_{n_w}$, and $\gamma_{\text{IQC}}^{(0)} := 1$ are also provided.

Each iteration starts with the construction of the scaled plant N_s , as described in section II-B. For the first iteration $N_s = \hat{N}$ given the initialization choices.

The next step is a nominal finite horizon synthesis for the scaled plant G_s under non-zero initial conditions. Here, the parameter variation ρ_Δ is treated as constant vector, with its entries chosen to the corresponding values of the uncertainty norm-bound b_ρ . Reference [14] provides necessary and sufficient conditions for the existence of a γ -suboptimal controller for non-zero initial conditions. Theorem 1 below is a special case of the results in [14].

Theorem 1: Consider an LTV system \hat{N} (11) with a fixed value of ρ_Δ , and $\gamma > 0$ given. Let Q be a given positive definite diagonal matrix. Let B , \hat{C} , \bar{R} and \hat{R} be defined as follows.

$$\begin{aligned} \hat{A} &:= \begin{bmatrix} A & 0 \\ 0 & 0 \end{bmatrix} & \hat{B} &:= \begin{bmatrix} Eb_\rho & B_d \end{bmatrix} \\ B &:= \begin{bmatrix} Eb_\rho & B_d & B_u \end{bmatrix} & \bar{R} &:= \text{diag}\{-\gamma^2 I_{n_w+n_d}, I_{n_u}\} \\ \hat{C} &:= \begin{bmatrix} 0 & C_e^T & C_y^T \\ 1^T & 0 & 0 \end{bmatrix}^T & \hat{R} &:= \text{diag}\{-\gamma^2 I_{n_v+n_e}, I_{n_y}\} \end{aligned}$$

- 1) There exists an admissible output feedback controller K such that $\|\mathcal{F}_l(\hat{N}, K)\|_{2[0, T]} < \gamma$ if and only if the following three conditions hold:

- a) There exists a differentiable function $X : [0, T] \rightarrow \mathbb{S}^n$ such that $X(T) = 0$,

$$\dot{X} + \hat{A}^T X + X \hat{A} - X B \bar{R}^{-1} B^T X + \hat{C}^T \hat{C} = 0$$

and $X(0) < \gamma^2 Q$.

- b) There exists a differentiable function $Y : [0, T] \rightarrow \mathbb{S}^n$ such that $Y(0) = Q^{-1}$,

$$-\dot{Y} + \hat{A} Y + Y \hat{A}^T - Y \hat{C}^T \hat{R}^{-1} \hat{C} Y + \hat{B} \hat{B}^T = 0$$

- c) $X(t)$ and $Y(t)$ satisfy the following point-wise in time spectral radius condition,

$$\rho(X(t)Y(t)) < \gamma^2, \forall t \in [0, T] \quad (13)$$

- 2) If the conditions above are met, then the closed loop performance $\|\mathcal{F}_l(\hat{N}, K)\|_{[0, T]} < \gamma$ is achieved by the central controller constructed from X and Y .

The reader is referred to [14] for the proof and technical assumptions on the structure of system matrices.

For a given value of $\gamma > 0$ and Q , the RDEs associated with X and Y are integrated backwards and forward in time, respectively. The diagonal entry in Q corresponding to x_ρ is chosen to one while all other entries are set to 10^6 . This choice of R renders system states x_Δ approximately zero and confines x_ρ to the set $\mathcal{U} := [-1, 1]$. If a solution to both RDEs exist and the condition $X(0) < \gamma^2 Q$ is fulfilled then the spectral radius coupling condition (13) is evaluated. The controller achieves the closed-loop performance γ if all conditions are fulfilled. A bisection yields the corresponding controller $K^{(i)}$.

Subsequently, the algorithm performs a robust performance analysis of the uncertain closed loop built from $N := \mathcal{F}_l(\hat{N}, K^{(i)})$ and ρ_Δ . The next Theorem 2 states a sufficient DLMI condition to upper bound the worst-case performance of an uncertain system $\mathcal{F}_u(N, \Delta)$ with non-zero initial conditions.

Theorem 2: Consider an LTV system N given by (1) and let $\Delta : \mathcal{L}_2^{n_v} [0, T] \rightarrow \mathcal{L}_2^{n_w} [0, T]$ satisfy the IQC defined by $M : [0, T] \rightarrow \mathbb{S}^{(n_v+n_w)}$. Assume $\mathcal{F}_u(N, \Delta)$ is well-posed. Let $Q : [0, T] \rightarrow \mathbb{S}^{n_\hat{x}}$, $S : [0, T] \rightarrow \mathbb{R}^{n_\hat{x} \times (n_w+n_d)}$, and $R : [0, T] \rightarrow \mathbb{S}^{(n_w+n_d)}$ be defined as follows.

$$\begin{aligned} D_v &:= \begin{bmatrix} D_{vv} & D_{vd} \end{bmatrix} & D_e &:= \begin{bmatrix} D_{ev} & D_{ed} \end{bmatrix} & \hat{Q} &:= C_e^T C_e, \\ S &:= C_e^T D_e, & R &:= D_e^T D_e - \gamma^2 \text{diag}\{0_{n_w}, I_{n_d}\} \end{aligned}$$

If there exists $\epsilon > 0$, $\gamma > 0$ and a differentiable function $P : [0, T] \rightarrow \mathbb{S}^{n_x}$ such that $P(T) \geq 0$, $P(0) < \gamma^2 Q$ and,

$$\begin{bmatrix} \dot{P} + A^T P + P A & P B \\ B^T P & 0 \end{bmatrix} + \begin{bmatrix} \hat{Q} & S \\ S^T & R \end{bmatrix} + \begin{bmatrix} C_v^T \\ D_v^T \end{bmatrix} M \begin{bmatrix} C_v^T \\ D_v^T \end{bmatrix}^T \leq -\epsilon I \quad (14)$$

then $\|\mathcal{F}_u(N, \Delta)\|_{2[0, T]} < \gamma$.

Proof: Theorem is a corollary of Theorem 6 in [13]. The proof provided in [13], which combines a standard dissipation argument [15]–[17] and IQCs, requires only minor modifications. ■

The IQC analysis step uses the algorithm proposed in [13] with an extension to uncertain initial conditions for the upper bound calculation. The same value for Q as in the synthesis is chosen, with the same implications. This algorithm returns the robust performance upper bound $\gamma_{\text{IQC}}^{(i)}$, and $M_v^{(i)}$ and $M_w^{(i)}$, which are used to build the scaled plant as described in section II-B. The algorithm commences with the next iteration and stops after a defined amount of iterations i_{max} .

V. NUMERICAL EXAMPLE: SPACE LAUNCHER

The numerical example concerns a robust pitch tracking control design for the rigid body motion of a Vega-like launch vehicle [18]. During the atmospheric ascent, the space launcher performs a gravity turn maneuver by tracking a pre-calculated pitch program. The gravity turn is the reference trajectory \mathcal{T} and assumes zero nominal wind, i.e., $w_{\mathcal{T}} = 0$. However, the launch performance is highly sensitive wind perturbations w_{Δ} . Their influence must be mitigated by the controller.

The launcher's nonlinear equations of motion are formulated with respect to its instantaneous center of gravity (CoG) G in a body-reference coordinate system and given by:

$$\begin{aligned} \ddot{\theta}(t) &= \frac{N(w, \dot{x}, \dot{z}, t) l_{GP}(t)}{J(t)} - \dot{\theta} \frac{\dot{J}(t)}{J(t)} \\ &\quad - \frac{T(t) l_{CG}(t)}{J(t)} \sin \delta_{\text{TVC}}(t) \\ \ddot{x}(t) &= \frac{T(t) \cos \delta_{\text{TVC}}(t) - A(w, \dot{x}, \dot{z}, t)}{m(t)} \\ &\quad - g_0 \sin \theta(t) - \dot{\theta}(t) \dot{z}(t) \\ \ddot{z}(t) &= - \frac{N(w, \dot{x}, \dot{z}, t)}{m(t)} - \frac{T(t)}{m(t)} \sin \delta_{\text{TVC}}(t) \\ &\quad + g_0 \cos \theta(t) - \dot{\theta}(t) \dot{x}(t) \end{aligned} \quad (15)$$

The variable θ denotes the pitch angle, while the axial and normal accelerations are denoted \ddot{x} and \ddot{z} . The variables A and N are the axial and normal aerodynamic acting on a time-dependent reference point P . Both forces depend nonlinearly on the wind velocity w (aligned with the z_b -axis), the forward velocity \dot{x} , \dot{z} , and time t . The launcher's time-dependent thrust T acts at the reference point C . It can be rotated by the angle δ_{TVC} using a thrust vector control (TVC) system. The overall moment of inertia J , mass m and CoG depend on time due to the thrust profile. The variables l denote the distance between reference points given in the subscript. Gravitational acceleration is denoted by g_0 .

While the launcher parameters are assumed known, the wind variation w_{Δ} along the reference trajectory \mathcal{T} is assumed ± 20 m/s uncertain. Hence, the wind variation is treated as an exogenous parameter ρ . Linearizing (15) about the gravity turn \mathcal{T} results in the LTV system:

$$\begin{bmatrix} \dot{\theta}_{\Delta} \\ \dot{\dot{\theta}}_{\Delta} \\ \dot{\dot{x}}_{\Delta} \\ \dot{\dot{z}}_{\Delta} \\ 0 \end{bmatrix} = \begin{bmatrix} 0 & 1 & 0 & 0 \\ 0 & -\frac{J_{\mathcal{T}}}{J_{\mathcal{T}}} & \frac{l_{GP\mathcal{T}}}{J_{\mathcal{T}} \dot{x}_{\mathcal{T}}} \frac{\partial N}{\partial \dot{z}} |_{\mathcal{T}} & \frac{l_{GP\mathcal{T}}}{J_{\mathcal{T}} \dot{x}_{\mathcal{T}}} \frac{\partial N}{\partial w} |_{\mathcal{T}} w_{\Delta} \\ -g_0 \sin \theta_{\mathcal{T}} & -\dot{x}_{\mathcal{T}} & -\frac{1}{m_{\mathcal{T}} \dot{x}_{\mathcal{T}}} \frac{\partial N}{\partial \dot{z}} |_{\mathcal{T}} & \frac{1}{m_{\mathcal{T}} \dot{x}_{\mathcal{T}}} \frac{\partial N}{\partial w} |_{\mathcal{T}} w_{\Delta} \\ 0 & 0 & 0 & 0 \\ 0 & -\frac{T_{\mathcal{T}} l_{CG\mathcal{T}}}{J_{\mathcal{T}}} & 0 & 0 \end{bmatrix} \begin{bmatrix} \theta_{\Delta} \\ \dot{\theta}_{\Delta} \\ \dot{x}_{\Delta} \\ \dot{z}_{\Delta} \\ x_{\rho} \end{bmatrix} + \begin{bmatrix} 0 \\ -\frac{T_{\mathcal{T}} l_{CG\mathcal{T}}}{J_{\mathcal{T}}} \\ -\frac{T_{\mathcal{T}}}{J_{\mathcal{T}}} \end{bmatrix} \delta_{\text{TVC}\Delta}. \quad (16)$$

The state \dot{x}_b has been truncated from the linear model following common practice in launcher pitch control design yielding a typical system order for launcher control designs, see, e.g., [19]. All entries in (16) are time-varying. The coefficients in (16) are calculated via numerical linearization for a time segment from 25 s to 80 s after lift-off, with a grid density of 0.25 s.

The robust control design requires a weighting structure to enforce meaningful closed loop requirements, such as tracking and limited control authority. A suitable (mixed-sensitivity) weighting structure for a space launcher is provided in [18] including tuning guidelines. The weighting scheme is depicted in Fig. 4.

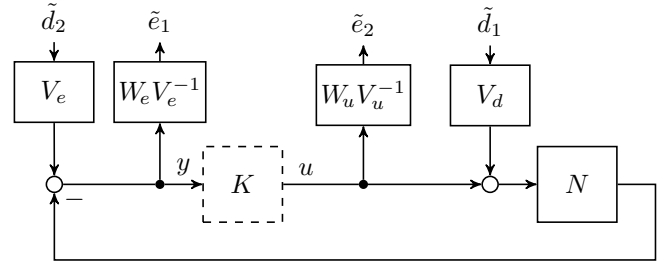


Fig. 4: Uncertain output feedback interconnection

The pitch angle θ and the pitch rate $\dot{\theta}$ are used as feedback signals. The weight W_e imposes tracking and disturbance rejection requirements. Here, θ shall be tracked up to a desired closed loop bandwidth of 0.75 rad/s. Thus, W_e is selected with integral behavior in the θ channel up to a frequency of 0.75 rad/s and a magnitude of 0.5 for robustness. A constant weight of 0.5 is selected in the $\dot{\theta}$ channel following the same reasoning. The weight W_u imposes control limitations and noise rejection requirements. To limit TVC activity to frequencies less than 10 rad/s, W_u is selected with unit magnitude up to 25 rad/s and differentiating behavior above 25 rad/s. The static weight V_e balances the two output errors. It is chosen as 1.0 deg for θ , 2.5 deg/s for $\dot{\theta}$. V_e specifies the available control effort against the chosen errors and is selected as 5 deg.

The controller is synthesized using Algorithm 1 with $N_{\text{syn}} = 4$ iterations. An updated version of the algorithm in [13] is used to perform the IQC analysis step with a tolerance of $5 \cdot 10^{-5}$, five iterations between the LMI and RDE solution, and 25 and 10 evenly spaced LMI and spline grid points on the considered time segment, respectively. The algorithm converged to a γ -value of 11.34. The synthesis required 1 h

and 45 min on a standard desktop computer with an Intel-Core i9 processor and 16 GB memory.

For comparison a nominal controller with non-zero initial conditions was synthesized following Theorem 1. The synthesis accounts for x_p . Instead of treating w_Δ as time-varying uncertainty, it is assumed with a fixed value of 20 m/s. Thus, the design only accounts for an (unknown) additional constant wind disturbance. The same weights W and V are used as in the robust synthesis.

Simulations are conducted in Matlab Simulink of the closed loops formed by nonlinear launcher dynamics and the nominal and the robust controller, respectively. Wind disturbance is injected into the system. It is constructed by superimposing the wind profile from Vega flight VV05 [20] with 1000 unique cases of severe Dryden turbulence [21]. Launcher certification processes commonly use turbulence models to account for uncertainty in wind estimations. Fig. 5 shows one of the injected wind profiles. Both controllers show no instability for these wind profiles. Fig. 6 depicts the resulting pitch error w.r.t. to the pitch program of the nominal (—) and robust closed loop (—) for the wind signal in Fig. 5. The turbulence component is then scaled up to assess the robustness of the designs. For a scaling-factor of 1.3, the robust controller failed to stabilize the system in 4% of the cases. The nominal controller failed 13%; about factor three worse. The unstable cases for the robust controller could be further reduced by increasing the uncertainty level. This was not pursued in the paper to uphold a fair comparison. Fig. 6 shows the closed loop behavior for the wind profile in Fig. 5 and a scaling of 1.3. The nominal controller becomes unstable (—), while the robust controller (—) can still stabilize the system and closely track the pitch profile. For this particular wind profile, a first instability occurs for a factor of 1.55 exceeding the nominal controller by 20%. In general, the robust controller demonstrates significantly increased robustness against fast-varying wind disturbances.

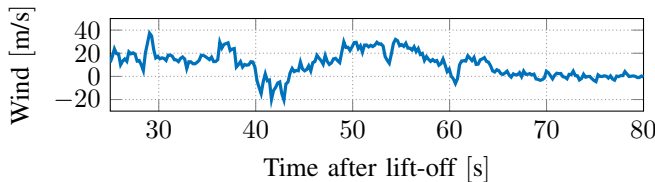


Fig. 5: Representative disturbance wind signal

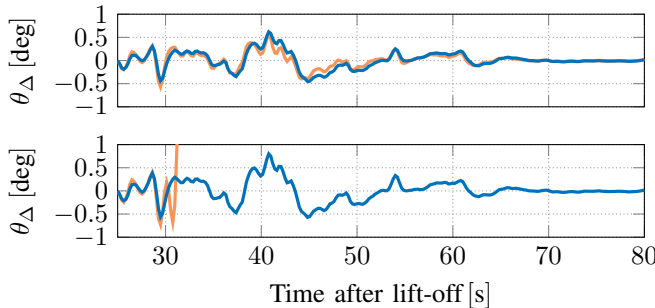


Fig. 6: Controller tracking performance for unscaled (top) and scaled disturbance (bottom): Robust (—); Nominal (—)

VI. CONCLUSION

The paper presents a novel approach for the synthesis of robust controllers for nonlinear systems along uncertain trajectories. It formulates time-varying parameter deviations from the nominal trajectory as uncertain initial conditions of an extended state space system in conjunction with time-varying uncertainties. The latter are bounded by integral quadratic constraints. Thus, the controller can be synthesized inside the LTV IQC framework. A realistic example demonstrates the capabilities of the approach.

REFERENCES

- [1] A. Hošovský, J. Piteř, K. Židek, M. Tóthová, J. Sárosi, and L. Cveticanin, "Dynamic characterization and simulation of two-link soft robot arm with pneumatic muscles," *Mech. and Mach. Theo.*, vol. 103, pp. 98–116, 2016.
- [2] F. Biertümpfel, S. Bennani, and H. Pfifer, "Time-varying robustness analysis of launch vehicles under thrust perturbations," *Adv. Contr. Appl.*, vol. 3, no. 4, 2021.
- [3] F. Capolupo and A. Rinalducci, "Descent and landing trajectory and guidance algorithms with divert capabilities for moon landing," in *AIAA SCITECH 2024 Forum*, 2024.
- [4] D. J. N. Limebeer, B. D. O. Anderson, P. P. Khargonekar, and M. Green, "A game theoretic approach to \mathcal{H}_∞ control for time-varying systems," *SIAM J. Control Optim.*, vol. 30, no. 2, pp. 262–283, 1992.
- [5] F. Biertümpfel, J. Theis, and H. Pfifer, "Observer-based synthesis of finite horizon linear time-varying controllers," in *2022 American Contr. Conf. (ACC)*, vol. 30. IEEE, 2022, pp. 2956–2961.
- [6] R. O'Brien and P. Iglesias, "Robust controller design for linear, time-varying systems," *Eur. J. Control*, vol. 5, no. 2-4, pp. 222–241, 1999.
- [7] C. Pirie and G. E. Dullerud, "Robust controller synthesis for uncertain time-varying systems," *SIAM J. Control Optim.*, vol. 40, no. 4, pp. 1312–1331, 2002.
- [8] M. Farhood and G. E. Dullerud, "Control of systems with uncertain initial conditions," *IEEE Trans. Autom. Contr.*, vol. 53, no. 11, pp. 2646–2651, 2008.
- [9] J. Buch and P. Seiler, "Finite horizon robust synthesis using integral quadratic constraints," *Int. J. Rob. Nonlin. Contr.*, vol. 31, no. 8, pp. 3011–3035, 2021.
- [10] F. Biertümpfel, J. Theis, and H. Pfifer, "Robustness analysis of nonlinear systems along uncertain trajectories," *IFAC-PapersOnLine*, vol. 56, no. 2, pp. 5831–5836, 2023.
- [11] P. Seiler, "Stability analysis with dissipation inequalities and integral quadratic constraints," *IEEE Trans. Autom. Contr.*, vol. 60, no. 6, pp. 1704–1709, 2015.
- [12] M. Green and D. J. N. Limebeer, *Linear Robust Control*. Upper Saddle River, NJ, USA: Prentice-Hall, Inc., 1995.
- [13] P. Seiler, R. M. Moore, C. Meissen, M. Arcak, and A. Packard, "Finite horizon robustness analysis of LTV systems using integral quadratic constraints," *Automatica*, vol. 100, pp. 135–143, 2019.
- [14] P. P. Khargonekar, K. M. Nagpal, and K. R. Poolla, " H_∞ control with transients," *SIAM J. on Control Optim.*, 1991.
- [15] J. C. Willems, "Dissipative dynamical systems part i: General theory," *Arch. for rat. mech. and analysis*, vol. 45, no. 5, pp. 321–351, 1972.
- [16] —, "Dissipative dynamical systems part ii: Linear systems with quadratic supply rates," *Arch. for rat. mech. and analysis*, vol. 45, no. 5, pp. 352–393, 1972.
- [17] D. J. Hill and P. J. Moylan, "Dissipative dynamical systems: Basic input-output and state properties," *J. of the Franklin Inst.*, vol. 309, no. 5, pp. 327–357, 1980.
- [18] F. Biertümpfel, H. Pfifer, and J. Theis, "Robust space launcher control with time-varying objectives," *J. Guid., Contr., Dyn.*, vol. 47, no. 5, pp. 934–944, 2024.
- [19] A. L. Greensite, "Analysis and design of space vehicle flight control systems. volume VII - attitude control during launch," NASA Marshall Space Flight Center; Huntsville, AL, Tech. Rep., 1967.
- [20] P. Simplicio, S. Bennani, A. Marcos, C. Roux, and X. Lefort, "Structured singular-value analysis of the vega launcher in atmospheric flight," *J. Guid., Contr., Dyn.*, vol. 39, no. 6, pp. 1342–1355, 2016.
- [21] F. M. Hoblit, *Gust Loads on Aircraft: Concepts and Applications*. American Institute of Aeronautics and Astronautics, 1988.